

# Microstructural Effects and the Toughening of Thermoplastic Modified Epoxy Resins

B.-G. MIN,<sup>1</sup> Z. H. STACHURSKI,<sup>1</sup> and J. H. HODGKIN<sup>2,\*</sup>

<sup>1</sup>Department of Materials Engineering, Monash University, Clayton, Vic. 3168, Australia;

<sup>2</sup>CSIRO, Division of Chemicals and Polymers, Clayton, Vic. 3168, Australia

## SYNOPSIS

We have studied an epoxy resin formulation consisting of the diglycidyl ether of bisphenol-A (DGEBA), modified with phenolic hydroxyl-terminated polysulfone (PSF) and cured with an aromatic amine curing agent, diaminodiphenyl sulfone (DDS). A range of microstructures and fracture properties have been obtained by controlling the formulation cure conditions (cure temperature and cure cycle in an isothermal mode). The chemical conversion of the cured resins has been monitored by near-infrared spectroscopy (NIR). Although only a single material formulation was used, three distinct types of microstructure were identified by scanning electron microscope (SEM) observations on samples prepared at different cure temperatures. Surprisingly, the thermal and fracture properties of the cured samples did not vary noticeably, in spite of the significant microstructure variations. The consistency of these fracture toughness results with cure temperature changes was an unexpected result in the light of our earlier observations of a strong dependence of fracture toughness on cure temperature in neat resin systems. The difference in behavior between neat and modified resins reveals that the fracture toughness of the latter is dependent on a combination of the microstructure and the matrix resin properties. This hypothesis was also supported by an observation of high fracture toughness in a sample cured in a two-step process, which we believe is due to the optimum microstructure and matrix resin properties, being achieved separately during precure and postcure, respectively. The increase in fracture toughness values caused by the modification ( $\Delta G_{IC}$ ) was calculated from the fracture toughness values of neat and modified resins, prepared under the same cure conditions, using a proposed theoretical equation. © 1993 John Wiley & Sons, Inc.

## INTRODUCTION

Regardless of the type of modifier, the system properties of modified epoxy resins are determined by two major factors: (i) the basic properties of the resin (matrix) as the bulk phase and (ii) the effect of the microstructure resulting from the presence of a second polymeric phase. These two factors are influenced concurrently by processing variables such as the matrix reactant ratios<sup>1-3</sup> and cure conditions.<sup>4-9</sup> In addition, the resultant microstructure is influenced by the concentration,<sup>9-13</sup> molecular weight,<sup>14</sup> and type<sup>15</sup> of the modifier. The influence

of changes in the material parameters make it difficult to investigate the toughening mechanism in a modified epoxy system even though the processing parameters used are consistent. With this in mind, a single modified epoxy system was employed in this study and the cure conditions were varied to obtain a range of microstructure and other related properties in the system free from the influences of the material parameters.

In our previous paper,<sup>4</sup> the mechanical behavior of an unmodified diglycidyl ether of bisphenol-A/diaminodiphenyl sulfone (DGEBA/DDS) resin system was investigated as a function of both cure temperature and cure cycle. In this article, the dependence of microstructure and fracture properties on cure temperature and cure cycle in a single PSF-modified epoxy system were studied under the same

\* To whom correspondence should be addressed.

cure conditions as employed in our study of the unmodified resin. These two studies allowed us to separate the contributions of microstructure and matrix to the final fracture toughness of the modified resin, using the following equation:

$$\Delta G_{IC} = G_{ICM} - G_{ICU}(1 - V_m) \quad (1)$$

where  $\Delta G_{IC}$  is the increase in fracture toughness due to modification;  $G_{ICM}$ , the fracture toughness of the modified resin;  $G_{ICU}$ , the fracture toughness of the unmodified resin (prepared under the same cure condition as the modified system), and  $V_m$ , the volume fraction of the modifier ( $V_m$  is managed to be constant [0.15] for all samples in this study). Volume fraction can be replaced by weight fraction since the densities of epoxy resin (1.235–1.237 g/cm<sup>3</sup>)<sup>4</sup> and PSF (1.24 g/cm<sup>3</sup> for  $M_n$  25000)<sup>15</sup> are very similar.  $\Delta G_{IC}$  represents contributions from many structural parameters, accompanying the modification. These structural parameters include (i) particle size,<sup>16</sup> (ii) volume fraction of the dispersed particles,<sup>17</sup> (iii) interfacial strength,<sup>18</sup> and (iv) the plastic deformation<sup>13</sup> in the matrix caused by the dispersed particles. All these parameters are related to the microstructure, formed by the addition of the modifier.

The toughening mechanism, as well as the optimum microstructure and cure condition, can be understood by correlating the calculated  $\Delta G_{IC}$  to the corresponding microstructure. The degree of toughening,  $Q$ , is defined as follows:

$$Q = \frac{G_{ICM} - G_{ICU}}{G_{ICU}} \times 100\% \quad (2)$$

## EXPERIMENTAL

### Materials

A diglycidyl ether of bisphenol-A (DGEBA) epoxy resin (Epikote 8283, Shell Chemicals, Australia,  $M_n$  380) and an aromatic amine curing agent 4,4'-diaminodiphenyl sulfone (DDS, Anchor Chemicals,  $M_n$  248) were used as the basic matrix materials. A low molecular weight ( $M_n$  10,000), phenolic hydroxyl-terminated polysulfone (PSF), was incorporated into the epoxy resin as a modifier.

### Synthesis of Polysulfone

The phenolic hydroxyl-terminated polysulfone of  $M_n$  10,000 was synthesized from bisphenol A and di-

chlorodiphenyl sulfone monomers by the conventional method described in detail by Johnson et al.<sup>19</sup> and Noshay et al.<sup>20</sup> The molar ratio of the reactant monomers, required for obtaining the final product with a desired molecular weight, was calculated according to the modified Carother equation.<sup>21</sup>

The final product was characterized by FTIR, DSC, and GPC. The number-average molecular weight of the PSF (determined by GPC measurement in tetrahydrofuran [THF]) was 10,000 g/mol ( $M_w/M_n = 2.58$ ), slightly lower than expected value of 11,000 g/mol. The glass transition temperature, obtained from DSC measurements using a scanning rate of 20°C/min, was 178°C.

### Modification and Curing

A mixture that contains stoichiometric (1 : 1) amounts of DGEBA and DDS in addition to 15 wt % (of total system) of PSF was prepared under vacuum in a rotary evaporator as follows: PSF, 7.155 g was dissolved in 25 mL of methylene chloride (CH<sub>2</sub>Cl<sub>2</sub>) and 30.4 g (0.08 mol) of DGEBA, and 2 mL of tetramethylammonium hydroxide catalyst (25% in methanol solution) was added. The 250 mL flask containing the mixture was connected to a rotary evaporator and evacuated to 30 mbar. The system was heated to 110°C rapidly by employing a preheated silicone oil bath and then further increased to 140°C for 30 min while the vacuum was increased slowly to 8 mbar. The system was held at that temperature for 30 min to allow prereaction between DGEBA and PSF. At this point, CH<sub>2</sub>Cl<sub>2</sub> was thought to have evaporated and the mixture that was initially a cloudy two-phase solution became a homogeneous semitransparent solution. The temperature was further increased to 165°C for 20 min to decompose the remaining catalyst and then reduced to 130°C. Next, 9.92 g (0.04 mol) of DDS was added slowly and the system was held at the above temperature until a homogeneous mixture was obtained (less than 30 min). The mixture was cast into a Teflon mold, preheated at the set cure temperature, and then cured isothermally in an air oven. The cure schedules employed in this study were either a one step cure: (i) 140°C for 6 h, (ii) 160°C, 6 h, (iii) 180°C, 6 h, (iv) 200°C, 6 h, or a two step cure: (v) 140°C for 2 h and then 180°C, 2 h.

### Testing Techniques

The infrared absorption spectra of the cured epoxy resins were recorded by an Alpha Centauri FTIR spectrometer (Mattson Instruments Inc., USA) in

the region from 11,000 to 4000  $\text{cm}^{-1}$  using 32 scans at a resolution of 8  $\text{cm}^{-1}$ . The chemical conversions of the functional groups of interest (epoxy, primary, and secondary amine groups) were obtained by the quantitative analysis methods reported in our previous paper.<sup>22</sup>

The thermal and mechanical properties such as glass transition temperature, flexural modulus, and fracture toughness were determined by the methods described in a previous publication.<sup>4</sup> The fracture surfaces were examined on a Jeol, JSM-840A, scanning electron microscope (SEM) at 20 kV. Prior to the examination, the surfaces were gold-coated using a high-vacuum gold sputterer to improve the surface conductivity.

## RESULTS AND DISCUSSION

### Chemical Conversion

The data showing conversion of epoxy group as a function of cure temperature are plotted in Figure 1. The conversion increased only 3% on increasing cure temperature from 140 to 160°C and then leveled off at 96% above 160°C, which is estimated to be the maximum conversion in the particular modified system employed (because of although the cure reaction may be delayed in the modified system, 6 h cure at high temperatures above 160°C is believed to be enough to arrest cure reaction even for the modified system when we consider our separate experimental observation that the vitrification time for neat resin system was 325 min at 130°C, 175 min

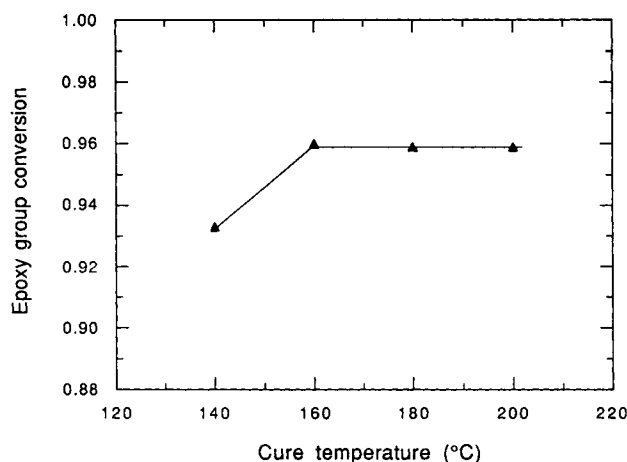


**Figure 1** Epoxy conversion vs. cure temperature as measured by near IR (PSF-modified epoxy resin, containing 15 wt % of  $M_n$  10,000 PSF; cure time 6 h).

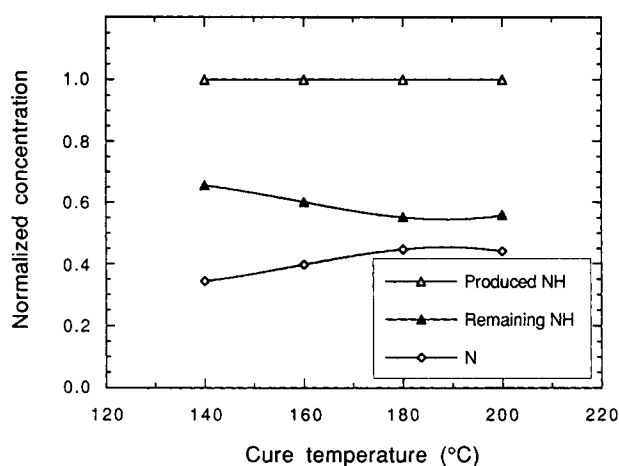


**Figure 2** Normalized concentrations of the secondary amine group (NH) and the tertiary amine groups (N) as measured by near IR (PSF-modified epoxy resin, containing 15 wt % of  $M_n$  10,000 PSF; cure time 6 h). Note that "N" = "produced NH" - "remaining NH."

at 160°C, 140 min at 190°C, and 141 min at 205°C). In another study of a stoichiometric DGEBA/DDS system,<sup>22</sup> we observed 100% maximum conversion. It is believed that the lower maximum conversion in this modified system is due to higher system viscosity during the cure, which will reduce the molecular mobility and, hence, will inhibit the reaction by diffusion control earlier than in the unmodified system.

The concentrations of the secondary and tertiary amine groups are shown (as normalized values) in Figure 2. About 55–65% of the secondary amine remained as unreacted species, although on average 96% of the epoxy groups were consumed. Theoretically, only 0.9% of the epoxy groups should be consumed by the reaction with the hydroxyl groups of the polysulfone modifier. Still, 22–27% of epoxy groups could be taken as the amount consumed by the side reactions such as homopolymerization and etherification reactions. These side reactions were not observed in stoichiometric neat resin systems,<sup>22</sup> but they were observed in nonstoichiometric neat resin systems and in modified systems.<sup>23</sup> It was proposed that the side reactions in the modified systems occur because of the restricted molecular mobility resulting from the increase of the system viscosity caused by the incorporation of PSF,<sup>23</sup> whereas the reaction by excess monomers in the later stage of the cure results in the side reactions in nonstoichiometric neat resin systems.

The normalized hydroxyl group concentrations, estimated separately from epoxy and amine group

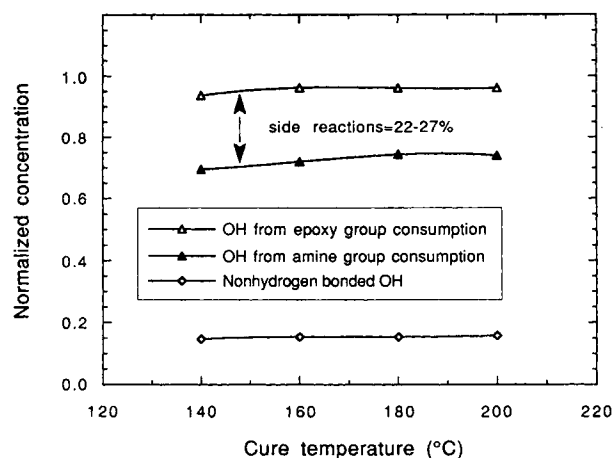


**Figure 3** Normalized concentration of hydroxyl groups vs. cure temperature for PSF-modified epoxy resin (15 wt % of  $M_n$  10,000 PSF; cure time 6 h). In the top two curves, each point was calculated from Figures 1 and 2 assuming that for every epoxy or amine group reacted there is one hydroxyl group produced. Also included was the initial concentration of hydroxyl groups. The data for the bottom curve were obtained directly by infrared measurement.

changes, are plotted, along with the normalized nonhydrogen-bonded hydroxyl-group concentrations as a function of cure temperature in Figure 3.

### Microstructures

SEM micrographs of fracture surfaces of the PSF-modified epoxy resins are presented in Figure 4 and show the dependence of the microstructure on the cure conditions. Figure 4(a)–(d) are the micrographs for the one-step cured samples, and Figure 4(e) is for the two-step cured sample.

It can be seen in Figure 4(a)–(d) that the microstructure varies noticeably with cure temperature changes. At the lowest temperature of 140°C, a phase-inverted structure was observed in many parts of the micrograph. It is shaped like a tree and has hard interconnected epoxy particles in the continuous PSF matrix. The typical particulate structure, which consists of dispersed PSF particles (0.1–0.2  $\mu\text{m}$  in diameter) in the epoxy matrix, covers the remaining parts of the micrograph. The phase-inverted microstructure was observed in earlier studies and attracted much interest as a structure that gave high fracture toughness properties. Yamanaka et al.<sup>7,8</sup> observed an interconnected globular structure in rubber and poly(ether sulfone) (PES)-modified epoxy systems, and this was considered to be a par-

ticular form of the phase-inverted structure. They concluded that the phase-separation mechanism in their systems was by spinodal decomposition.

At 160°C [Fig. 4(b)], the normal particulate structure is no longer observed; instead, a phase-inverted structure (with hard epoxy particles in 0.7–1.0  $\mu\text{m}$  diameter PSF-rich inclusion) is found throughout the micrograph picture. At 180°C [Fig. 4(c)], only the particulate structure is observed. In this case, the PSF particles are about 0.1  $\mu\text{m}$  in diameter, the smallest size observed in this study, although the density of the particles was the greatest. At the maximum cure temperature, 200°C [Fig. 4(d)], the structure is similar to that of the sample cured at 180°C but the particle size increased to 0.2–0.4  $\mu\text{m}$  and the density of particles was lower. The tendency of the particle size to increase at high cure temperatures is in agreement with the reports by Manzione and Gillham<sup>5,6</sup> and others<sup>24</sup> in their 10% carboxyl-terminated butadiene acrylonitrile (CTBN) rubber-modified DGEBA/piperidine epoxy system.

It is noteworthy that the sample cured in a two-step cure cycle [Fig. 4(e)] has a similar microstructure to that of the sample cured in one step 140°C cure procedure, shown in Figure 4(a). The two-step microstructure consists of the particulate phase, which has PSF particles of 0.4–0.5  $\mu\text{m}$  diameter in the epoxy matrix, and a phase-inverted structure, larger than that for the 140°C cured sample. This result implies that the final microstructure of the modified resin is strongly dependent on the first cure temperature rather than on the postcure temperature, when it is cured by this two-step cycle. This important observation has also been reported in rubber-modified epoxy systems.<sup>5,6</sup>

The phase-inverted structure was confirmed by observations on samples “etched” by methyl ethyl ketone (MEK) for 30 days.<sup>23</sup> The cured epoxy is insoluble in MEK, whereas PSF is quite soluble. The interconnected particles (epoxy) in the phase-inverted phases were not damaged at all, while the co-continuous matrix (PSF) was dissolved.

### Glass Transition Temperature

The variation of the glass transition temperature ( $T_g$ ) of the samples cured in both the one-step and two-step cycles is shown in Figure 5 and Table I, respectively. For all samples, a single  $T_g$  was observed from DMTA measurement. Note that the  $T_g$  of the PSF-modified resin was not influenced by cure temperature and cure cycle except that cured at

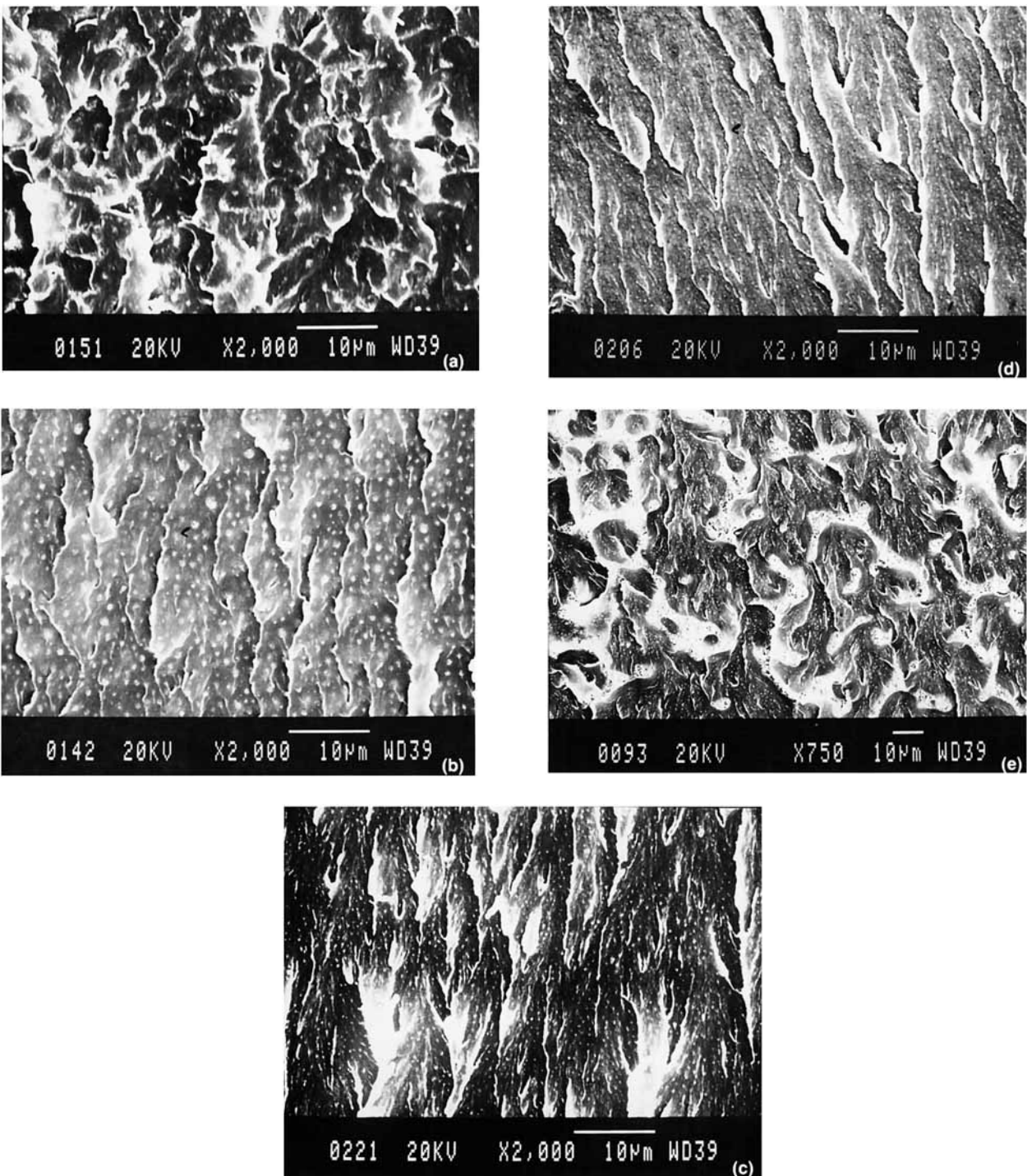


**Figure 4** SEM micrographs of fracture surfaces of a PSF-modified formulations (15 wt % of  $M_n$  10,000 PSF), showing the variation of microstructure under different cure conditions: (a) 140°C, 6 h; (b) 160°C, 6 h; (c) 180°C, 6 h; (d) 200°C, 6 h; (e) 140°C, 2 h/ 180°C, 2 h.

140°C which had a lower degree of epoxy conversion ( $T_g$  is proportional to the degree of epoxy conversion). In unmodified resin systems, the glass trans-

sition temperature increased linearly toward its  $T_{g\infty}$  with increasing final cure temperature, regardless of cure cycle.<sup>4</sup> The reason for this tendency of the  $T_g$

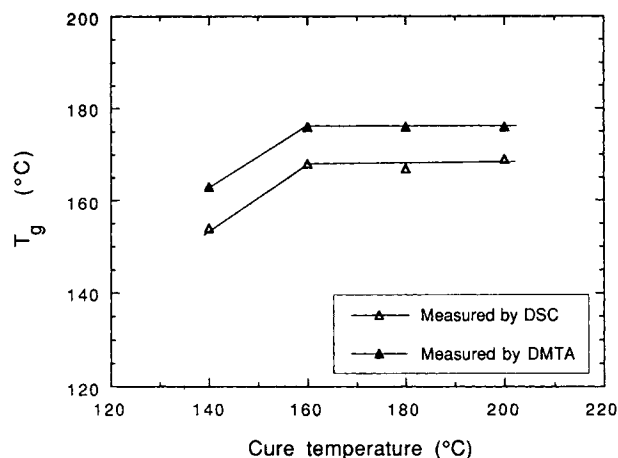


**Figure 5** Glass transition temperatures for PSF-modified epoxy resin (15 wt % of  $M_n$  10,000 PSF) plotted against cure temperature (cure time 6 h).

in the PSF-modified system is not clear, but it is assumed to be due to the combination of factors: (i) the epoxy resin that increases the  $T_g$  with increasing cure temperature and (ii) the PSF dissolved in the epoxy that is believed to decrease the  $T_g$  of the system by plasticizing the matrix resin.

**Table I** Chemical Conversions and Thermal and Fracture Properties of a Two-step Cured PSF-modified Epoxy Resin (Containing 15 Wt % of  $M_n$  10,000 PSF); Cure Cycle 140°C for 2 h/180°C for 2 h

Epoxy conversion	0.96
Normalized concentration of produced secondary amine groups	1.00
Normalized concentration of remaining secondary amine groups	0.58
Normalized concentration of tertiary amine groups	0.42
Normalized concentration of hydroxyl groups	
Estimated from epoxy group consumption	0.96
Estimated from amine group consumption	0.73
Nonhydrogen-bonded	0.16
Glass transition temperature (°C)	
From DSC	171
From DMTA	176
Flexural modulus (GPa)	3.00
Flexural strength (MPa)	109
Critical stress intensity factor, $K_{IC}$ ( $MN\ m^{-3/2}$ )	1.01
Critical strain energy release rate, $G_{IC}$ ( $J/m^2$ )	309
Fracture toughness caused by the modification, $\Delta G_{IC}$ ( $J/m^2$ )	226
Degree of toughening, $Q$ (%)	215

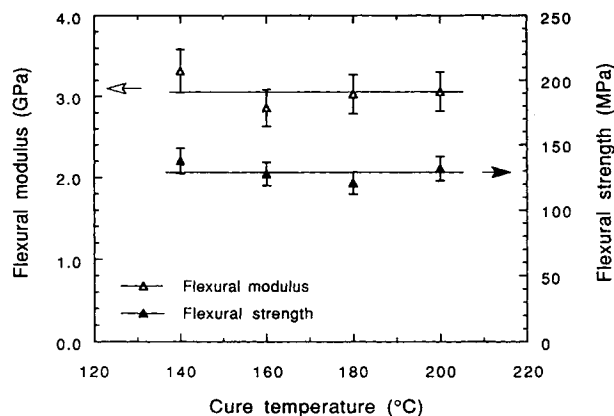


**Figure 6** Flexural modulus and strength for PSF-modified epoxy resin (15 wt % of  $M_n$  10,000 PSF) plotted against cure temperature (cure time 6 h).

### Mechanical Properties

The flexural modulus and flexural strength of the PSF-modified formulation, shown in Figure 6, did not vary in the range of cure temperatures and cure cycles employed in this study, except that the flexural strength for the sample cured in the two-step cure profile showed a slightly lower value. The lack of significant variation in the flexural modulus is quite similar to that observed in unmodified system in our previous study.<sup>4</sup> This consistent trend implies that the microstructure does not affect the modulus of a particular PSF-modified resin formulation.

The fracture toughness, indicated by both the critical stress intensity factor,  $K_{IC}$ , and the critical strain energy release rate,  $G_{IC}$ , are presented in Figure 7 for one-step cured samples and in Table I for the two-step cured sample. The value for the two-

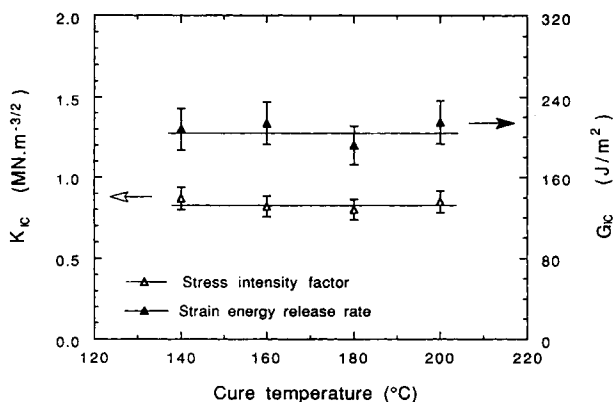


**Figure 7** Fracture toughness as shown by the stress-intensity factor and strain energy release rate for PSF-modified epoxy resin (15 wt % of  $M_n$  10,000 PSF) plotted against cure temperature (cure time 6 h).

step cured sample is much higher than any of the single-step cured samples. For the latter samples, this fracture toughness value was not dependent on cure temperature, unlike the tendency that we previously observed in unmodified resin systems<sup>4</sup> (where it increased linearly as the cure temperature increased). These observations indicate that the microstructure is another important factor, which determines the fracture properties of the modified resin. The lack of change in fracture toughness with cure temperature increases (in the single-cure-step system) implies that (i) the microstructure and matrix resin properties are influenced by cure temperature in opposite ways and (ii) the structure observed at low temperature is the optimum structure, but the matrix properties achieved at high temperature are desirable for obtaining the maximum toughness value in this particular modified system employed. This conclusive phenomenon is reflected in the fracture toughness of the two-step cured sample that obtained its optimum structure during the precure at low temperature and achieved high matrix resin properties during the high-temperature post-cure.

### Structure—Degree of Toughening

The conclusions reached above can also be supported by separately calculating the contributions to fracture toughness due to (i) the microstructure and (ii) the matrix resin, using eqs. (1) and (2).

The fracture toughness of the unmodified resin ( $G_{ICU}$ ),<sup>4</sup> that of the PSF-modified resin ( $G_{ICM}$ ), and the fracture toughness enhancement due to PSF

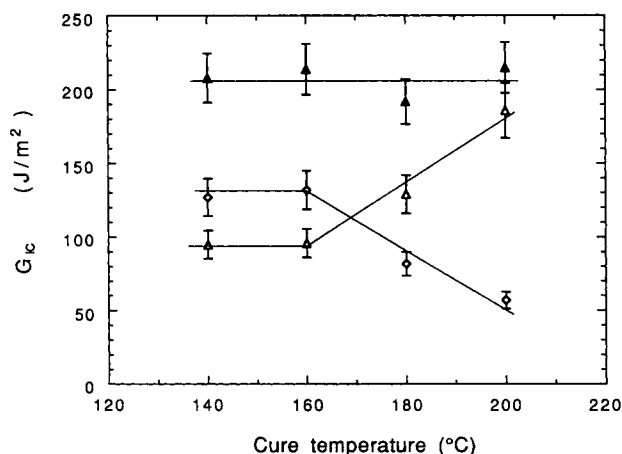


**Figure 8** Fracture toughness vs. cure temperature for ( $\Delta$ ) unmodified epoxy resin and ( $\blacktriangle$ ) PSF-modified epoxy resin (15 wt % of Mn 10,000 PSF). ( $\diamond$ ) is the fracture toughness enhancement due to PSF modification.

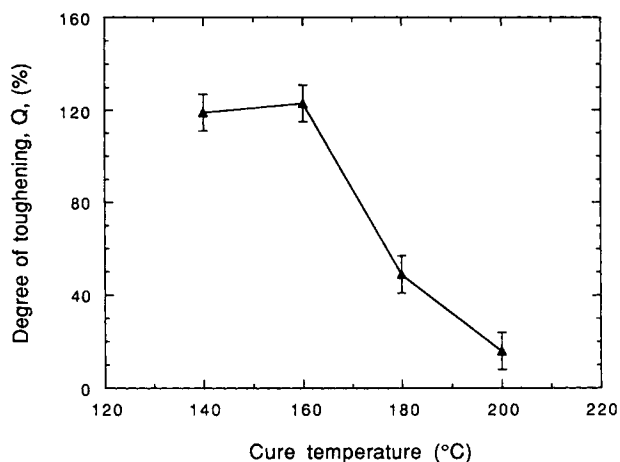


**Figure 9** Degree of toughening,  $Q$ , vs. cure temperature for PSF-modified epoxy resin (15 wt % of Mn 10,000 PSF; cure time 6 h).

modification ( $\Delta G_{IC}$ ) are shown in Figure 8. Maximum  $\Delta G_{IC}$  was obtained from the samples cured at the lower temperatures (140 and 160 $^{\circ}C$ ) and these had large amounts of phase-inverted phases. As the microstructure changed to more particulate forms (with increasing cure temperature),  $\Delta G_{IC}$  decreased significantly to less than one-third of the corresponding  $G_{ICU}$  (at 200 $^{\circ}C$  cure). Meanwhile, the  $\Delta G_{IC}$  value for the two-step cured sample, shown in Table I, was significantly enhanced when compared to that of the one-step cured samples. Since  $\Delta G_{IC}$  was defined as the value of the contribution of the particular microstructure, we can decide on the optimum microstructure and further understand the toughening mechanism by comparison of the microstructure to the corresponding  $\Delta G_{IC}$ . The phase-inverted structure that gives higher  $\Delta G_{IC}$  is considered as an optimum microstructure in the range of this study and the value of  $\Delta G_{IC}$  is believed to increase proportionally with the portion of the phase of the structure. In addition, a large amount of ductile tearing in the continuous PSF matrix was observed, whereas only the shear banding, interconnecting the PSF particles, was observed in detailed examinations of the SEM pictures of the particulate structure phase. These two observations also suggest that the main toughening mechanism in this particular PSF-modified resin system is the ductile tearing of continuous PSF phases. The shear banding, caused by dispersed PSF particles, is a minor factor for toughening. The degree of toughening,  $Q$ , calculated using eq. (2) is presented in Figure 9 and Table I. The value varies from 15% at 200 $^{\circ}C$  for the one-step cure to 215% for the two-step cure.

From the above observations, we can define the optimum cure condition for the particular modified system. The two-step cure profile, which can arrest an optimum structure during low-temperature precure and can achieve high matrix resin properties during high-temperature postcure, is considered as an optimum cure condition in the range of this study.

## CONCLUSIONS

The microstructural effects on the total fracture toughness and the toughening mechanisms in PSF-modified resin systems can be studied by comparing the fracture toughness of the unmodified resin system<sup>4</sup> and the microstructure and fracture toughness of the modified resin system under the same cure conditions. An analysis of these fracture toughness values, using a proposed theoretical equation, has allowed us to separate the contributions of the microstructure and the matrix resin fracture property to the final fracture toughness of the modified resin. Although the microstructure changed significantly as the cure temperature increased, the fracture toughness of the modified resin remained essentially constant. Nevertheless, the microstructural contribution to the fracture toughness and the calculated degree of toughening rapidly decreased with the diminishing area of the phase-inverted co-continuous structure, which was believed to be an optimum microstructure for toughening. In addition, it was observed, from the comparison of the microstructures to their corresponding  $\Delta G_{IC}$ , that the main toughening mechanism in this PSF-modified resin system is ductile tearing occurring in co-continuous PSF matrix.

One of the authors (B.-G. M.) would like to thank CSIRO for financial support during the work.

## REFERENCES

1. C. D. Wingard and C. L. Beatty, *J. Appl. Polym. Sci.*, **41**, 2539 (1990).
2. S. C. Misra, J. A. Manson, and L. H. Sperling, in *Epoxy Resin Chemistry*, R. S. Bauer, Ed., ACS Symposium Series 114, American Chemical Society, Washington, DC, 1979, p. 157.
3. J. Mijovic and L. Tsay, *Polymer*, **22**, 902 (1981).
4. B.-G. Min, J. H. Hodgkin, and Z. H. Stachurski, *J. Appl. Polym. Sci.*, to appear.
5. L. T. Manzione and J. K. Gillham, *J. Appl. Polym. Sci.*, **26**, 907 (1981).
6. L. T. Manzione and J. K. Gillham, *J. Appl. Polym. Sci.*, **26**, 889 (1981).
7. K. Yamanaka, Y. Takagi, and T. Inoue, *Polymer*, **60**, 1839 (1989).
8. K. Yamanaka and T. Inoue, *Polymer*, **30**, 662 (1989).
9. D. Verchere, J. P. Pascault, H. Sautereau, S. M. Moschiar, C. C. Riccardi, and R. J. J. Williams, *J. Appl. Polym. Sci.*, **42**, 701 (1991).
10. J. N. Sultan, R. C. Laible, and F. J. McGarry, *Appl. Polym. Symp.*, **16**, 127 (1971).
11. J. C. Hedrick, D. A. Lewis, T. C. Ward, and J. E. McGrath, *Polym. Prepr.*, **29**(1), 363 (1988).
12. D. J. Hourston and J. M. Lane, *Polymer*, **33**, 1379 (1992).
13. W. D. Bascom, R. L. Cottingham, R. L. Jones, and P. Peyser, *J. Appl. Polym. Sci.*, **19**, 2545 (1975).
14. J. L. Hedrick, I. Yilgor, G. L. Wilkes, and J. E. McGrath, *Polym. Bull.*, **13**, 201 (1985).
15. A. H. Gillham, PhD Thesis., Cranfield Institute of Technology, U.K., 1988.
16. S. C. Kunz, J. A. Sayre, and R. A. Assink, *Polymer*, **23**, 1897 (1982).
17. S. Kunz-Douglass, P. W. R. Beaumont, and M. F. Ashby, *J. Mater. Sci.*, **15**, 1109 (1980).
18. L. C. Chan, J. K. Gillham, A. J. Kinloch, and S. J. Shaw, in *Rubber-Modified Thermoset Resins*, C. K. Riew and J. K. Gillham, Eds., Adv. Chem. Ser. 208, American Chemical Society, Washington, DC, 1984, p. 195.
19. R. N. Johnson, A. G. Farnham, R. A. Clendinning, W. F. Hale, and C. N. Merriam, *J. Polym. Sci. Part A-1*, **5**, 2375 (1967).
20. A. Noshay, M. Matzner, and C. N. Merriam, *J. Polym. Sci. Part A-1*, **9**, 3147 (1971).
21. G. Odian, *Principles of Polymerization*, 2nd ed., Wiley-Interscience, New York, 1981, p. 113.
22. B.-G. Min, Z. H. Stachurski, J. H. Hodgkin, and G. R. Heath, *Polymer*, to appear.
23. B.-G. Min, J. H. Hodgkin, and Z. H. Stachurski, *J. Appl. Polym. Sci.*, to appear.
24. G. Levita, in *Rubber-Toughened Plastics*, C. K. Riew, Ed., Adv. Chem. Ser. 222, American Chemical Society, Washington, DC, 1989, p. 93.

Received January 20, 1993

Accepted April 2, 1993